small
NANO MICRO
www.small-journal.com

Stretchable and Energy-Efficient Heating Carbon Nanotube Fiber by Designing a Hierarchically Helical Structure

Peng Liu, Yiming Li, Yifan Xu, Luke Bao, Lie Wang, Jian Pan, Zhitao Zhang, Xuemei Sun, and Huisheng Peng**

Inspired by the hierarchically helical structure of classical thermal insulation material—wool, a stretchable heating carbon nanotube (CNT) fiber is created with excellent mechanical and heating properties. It can be stretched by up to 150% with high stability and reversibility, and a good thermal insulation is achieved from a large amount of formed hierarchically helical voids inside. Impressively, it exhibits ultrafast thermal response over 1000 °C s^{-1}, low operation voltage of several volts, and high heating stability over 5000 cycles. These hierarchically helical CNT fibers, for the first time, are demonstrated as monofilaments to produce soft and lightweight textiles at a large scale with high heating performances.

Over millions of years of evolution, nature creatures have formed various unique structures which contribute to intriguing functionalities.[1,2] One such extraordinary structure is the helical structure present in many different species and scales, from microscopic DNA, bacterial flagella and viral capsids to macroscopic seed pods, plant vasculatures, and tendrils.[3] Inspired by these natural helical structures and their functionalities, a lot of materials and devices had been made into helical structures with different functionalities for various applications, such as microelectronics, micromechanics, optics, sensing, and biomedicine.[4–6] However, it is rare to enhance heating effects by designing helical structures, although the wool fibers just provide a promising paradigm on how the helical structure keeps warm efficiently. For instance, sheep wool represents a widely used thermal insulation material in the garment industry based on a hierarchically helical structure. As shown in **Figure 1**a,b,[7] the twisted keratin molecules (protein chains) are coiled in a helical structure like a spring and form microfibrils in the matrix, bundles of microfibrils make up longer macrofibrils, and the hierarchical fibrils and matrix cells finally produce the hierarchically helical wool fiber. The helical coil—the smartest part of the fiber—offers the wool with a superior thermal insulation property as well as a combined high flexibility, elasticity, and resilience.

However, reducing heat dissipating to keep warm like woolen textile is passive and not enough, especially under extreme circumstances, so active heating had been proposed to keep the body warm as well as many other application fields such as human healthcare,[8] automobile defogging,[9] and controlled drug delivery.[10] Three classes of materials and their composites are mainly used for the Joule heat generation, i.e., metal,[11,12] carbon,[13,14] and conductive polymer.[15,16] Metals were designed into wavy patterns or metal nanowires were embedded into elastomeric matrices for stretchable and transparent heaters.[17,18] Conductive polymers like poly(3,4-ethylenedioxythiophene) possessed some merits like easy processing and mass production.[15] Carbon-based materials, e.g., graphene and carbon nanotube (CNT), had been made into different forms and showed advantages of light weight, flexibility, high mechanical strength, high electrical conductivity, and good thermal stability.[19–25] Unfortunately, the available heaters were typically made into films that are not soft, breathable, and washable, which were unable to meet the requirements of many heating appliations like woolen textiles. For instance, they could not satisfy a broad spectrum of booming fields such as portable and wearable electronics.

In this Communication, inspired by the wool fiber, we created an aligned CNT fiber with high mechanical and thermal properties by designing a hierarchically helical structure. Just like the wool fiber (Figure 1a,b), the CNT fiber was also composed of a fundamental fiber unit—CNT, which made up the helical primary fiber, and then bundles of primary fiber constituted the hierarchically helical fiber (HHF). The aligned structure had effectively extended the remarkable properties of CNT that were critical for heaters to the microsized fiber. In particular, the hierarchically helical structure offered the aligned CNT fiber with high stretchability without sacrificing the high electrical conductivity, which remains challenging for the conventional stretchable heating films by embedding conductive nanomaterials into insulating elastomeric matrix.[26,27] More important, the formed hierarchically helical voids inside the CNT fiber offered a good thermal insulation property like wool fiber. These CNT fibers had been further woven into heating textiles that presented softness, toughness, ultrafast thermal response, and low operation voltage.

Dr. P. Liu, Y. Li, Y. Xu, L. Bao, L. Wang, J. Pan, Dr. Z. Zhang, Dr. X. Sun, Prof. H. Peng
State Key Laboratory of Molecular Engineering of Polymers
Department of Macromolecular Science
Laboratory of Advanced Materials
Fudan University
Shanghai 200438, China
E-mail: sunxm@fudan.edu.cn; penghs@fudan.edu.cn

DOI: 10.1002/smll.201702926

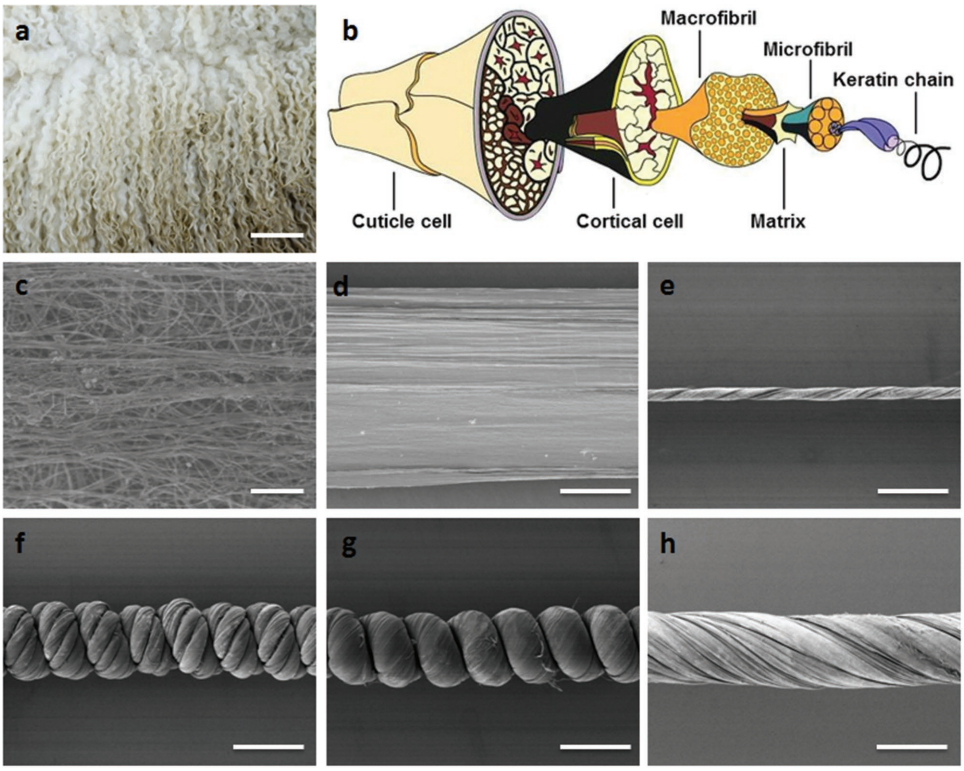

Figure 1. a) Photograph of wool. b) Schematic illustration to the hierarchically helical structure of wool fiber. c,d) Scanning electron microscope (SEM) images of CNT ribbon at high and low magnifications, respectively. e) SEM image of primary CNT fiber. f–h) SEM images of HHF, SSF, and SNF with the same diameter. Scale bars, 3 cm in (a), 1 µm in (c), and 200 µm in (d–h).

The HHF was prepared by twisting CNT ribbons (Figure 1d) that were synthesized through floating catalyst chemical vapor deposition.[28] The diameters of CNTs were around 20 nm, and they had been aligned along the ribbon length to produce plenty of nanoscaled voids among them (Figure 1c). The CNT ribbons were pulled out of the furnace with a width of 500 µm and then pretwisted to form the primary CNT fiber with a diameter of ≈50 µm (Figure 1e). Accordingly, the nanoscale voids evolved into a helical structure with the size ranging from ≈10 to 100 nm (Figure S1, Supporting Information). A bundle of ten primary fibers had been further twisted together (Figure S2, Supporting Information), and helical micrometer-scaled voids with the average size of ≈8 µm were thus generated among neighboring primary fibers (Figure S3, Supporting Information). After the formation of helixes along the whole fiber, the resulting HHF displayed a diameter of ≈220 µm, and larger helical micrometer-scaled voids with the average size of ≈12 µm were produced among the neighboring helixes (Figure 1f and Figure S4, Supporting Information). In other words, three levels of aligned helical voids had been prepared by this preparation strategy that may be extended to the other 1D nanomaterials. As a comparison, single-ply spring-like fiber (SSF, Figure 1g) and single-ply nonspring-like fiber (SNF, Figure 1h) with the same diameter as HHF were twisted from stacked multilayered CNT ribbons for the following control study.

These fiber materials possessed high electrical conductivity of appropriately 7.4×10^2 S cm^{-1} and low density of appropriately 0.615 g cm^{-3}, which were critical for heating applications. Their Joule heating properties were first studied by tracing the temperature over time of the HHF (**Figure 2**a). When a voltage was applied on its two ends (length of 2 cm), it generated heat immediately and reached saturated temperature in a moment. So did the SSF and SNF on the thermal response. Along with the increasing input voltages from 2, 3, and 4 to 5 V, the saturated temperatures rose from 55, 76, and 103 to 135 °C (Figure 2b). Furthermore, the saturated temperature can be improved by twisting a number of fibers together because the increased diameter leads to higher current-carrying capacity. For instance, a multiply fiber (length of 2 cm) twisted from 32 primary fibers with a diameter of ≈500 µm produced much higher saturated temperature of 459 °C at a voltage of 1.7 V (Figure S5, Supporting Information). Besides, the saturated temperature had been well maintained for the HHF during 5000 ON/OFF cycles (Figure 2c). Importantly, the high heating performance had also been well maintained under deformations like bending and torsion (Figure S6, Supporting Information).

The HHFs also showed ultrafast thermal response (Figure S7, Supporting Information), and the maximal heating rate rose with increasing voltages and reached up to 1030 °C s^{-1} at a low voltage of 8 V. This remarkably fast responding behavior was attributed to their high thermal conductivity,[29] ultrasmall heat capacity per unit volume, and large specific surface area.[30] The cooling rate represented the thermal insulation property of a material, so the SNF, SSF, and HHF with the same length (2 cm) and diameter (220 µm) were heated to 80 °C

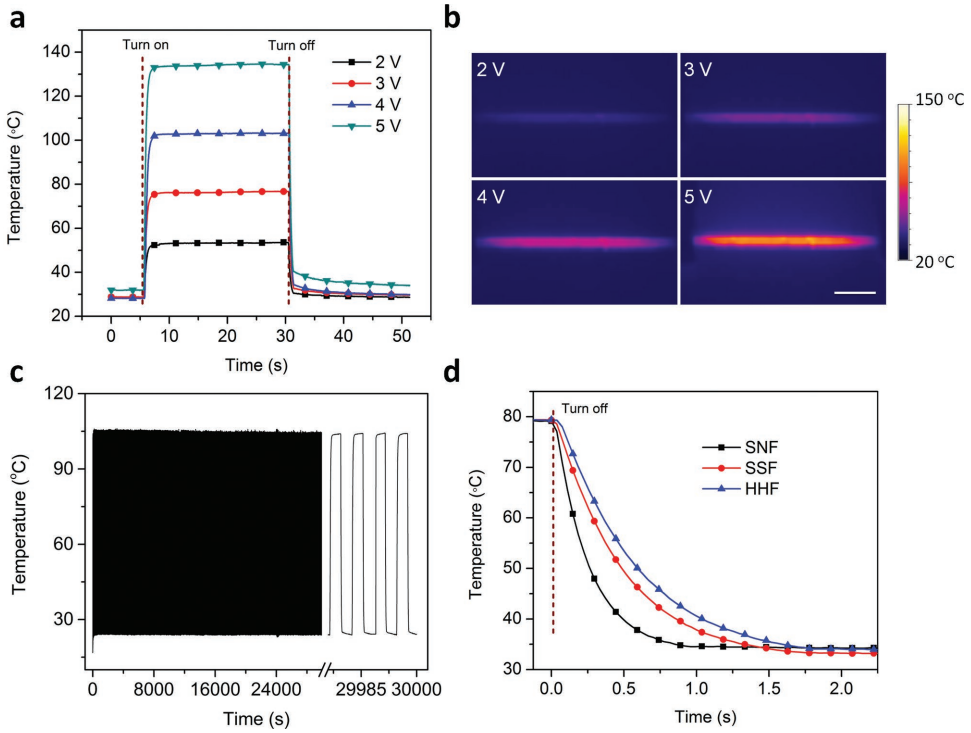

Figure 2. Joule heating characterization of the HHF. a) Temperature–time curves at voltages of 2, 3, 4, and 5 V. b) Infrared images at 2, 3, 4, and 5 V. c) Temperature–time curve under pulsed voltages between 0 and 4 V for 5000 cycles. d) Cooling curves of HHF, SSF, and SNF from about 80 °C. Scale bar, 5 mm in (b).

and then the input voltages were turned off at the same time to compare their cooling curves (Figure 2d). Since the thermal conductivity of CNT fiber (25 W m^{-1} K^{-1}) was much higher than that of air (0.02–0.03 W m^{-1} K^{-1}),[29] the HHF with the most void per unit volume demonstrated the lowest cooling rate, while the SNF with the least void showed the highest cooling rate. Meanwhile, the input power also reflected the heating efficiency. To maintain the high temperature of three fibers at 80 °C, the input power for HHF, SSF, and SNF were 0.30, 0.35, and 0.47 W, respectively. Therefore, the HHF saved energy by 14% and 36% compared with the SSF and SNF, mainly due to the hierarchically helical void structure. The different diameters of three families of fibers were also investigated on the cooling rate (Figure S8, Supporting Information). The same trend occurred, i.e., the HHFs produced lower cooling rates than SSFs and SNFs. Note that larger HHFs could save relatively more energy, e.g., an HHF twisted from 15 primary fibers (diameter of 290 μm) saved 43% compared with an SNF with the same diameter.

The HHF exhibited a tensile strength of 159 MPa and elongation at breaking up to 150% due to the elasticity of the twisted helixes (Figure S9, Supporting Information). The length of the HHF (2 cm) was about one quarter of its initial length (7.5 cm) after twisting, meanwhile the resistance decreased obviously (i.e., from 37 to 26 Ω). The decreased resistance was originated from the contacts of adjacent helixes, leading to some unique and interesting properties during stretching. As shown in **Figure 3**a, the resistance of the HHF increased remarkably by 30% within the first 40% strain due to the detaching of adjacent helixes; in the rest deformation up to 150% before fracture, the resistance only increased by 10%, because the deformation was more obvious by stretching the helix into line at this stage. The process was verified by temperature profile under stepwise strain of the HHF during stretching (Figure 3b) and had been further clearly observed from the optical images (Figure 3c). At a constant voltage, the temperatures of the HHF dropped dramatically by 35 °C within the beginning 40% strain and only 15 °C within the rest strain up to 140%. The resistance evolution of the HHF was also traced under 40% strain for 100 stretching/releasing cycles (Figure 3d). For the first cycle, the resistances were increased due to the releasing of stress (Figure S10, Supporting Information), and then it remained stable during the following cycles.[11,26,31]

To compare, the HHFs demonstrated promising advantages over the other heating materials (**Figure 4**). They were safe without toxic components, their density of 0.615 g cm^{-3} was lower than common chemical fibers (e.g., 1.15 g cm^{-3} for nylon), and their specific strengths were higher than the strongest commercial fiber of T1000 (a carbon fiber material).[32] They possessed ultrafast thermal responses up to 1030 °C s^{-1}, which was much higher than previous resistive heaters based on metal, polymer, and carbon nanomaterials (Table S1, Supporting Information), e.g., commercial Kanthal heating wire (29.1 °C s^{-1}) and graphene fiber (571 °C s^{-1}),[13,33] so they displayed much higher sensitivity and speedy start. The high temperature resistance (over 450 °C) and heating stability (over 5000 ON/OFF cycles) were also advantageous as some heating materials like metals would be oxidized easily.[13,34–36] The high stretchability of the HHF exceeded 80%, which was promising for a variety of applications that need intimate contacts with

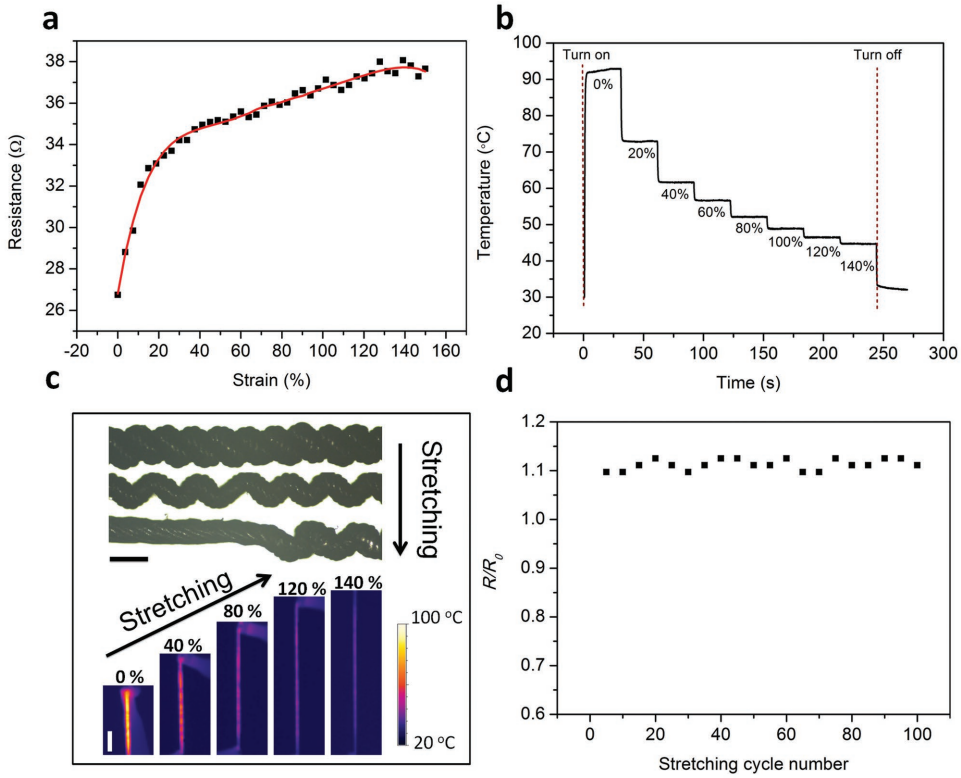

Figure 3. Stretchable characterization of the HHF. a) Dependence of electrical resistance on strain. b) Temperature profile under stepwise strain at 3.5 V. c) Optical images and infrared images during stretching. Scale bars, 200 µm (top) and 1 cm (bottom). d) Relative resistances under stretching/releasing process for 100 cycles at a strain of 40%. R_0 and R correspond to the resistances before and after stretching, respectively.

curvilinear surfaces.[13,37] The thermal insulation property of the HHF made it energy efficient for heating.

These fiber materials had been thus woven with cotton threads and copper wires to prepare heating textiles (**Figure 5**a). The cotton threads served as supporting substrates, and the copper wires were directly woven into the textile as the conductors without using any conductive paste or tape, so no more post-treatments were needed, which favored large-scale fabrication and enhanced washability (Figure 5b). This textile model exhibited a large heating area of 13 × 10 cm^2. When it was subjected to increasing voltages from 5 and 7 to 9 V, the saturated temperatures rose from 38 and 48 to 60 °C (Figure 5c), and the temperature distribution was uniform without blind spots throughout the heating textile (Figure S11, Supporting Information). As presented in Figure 5d, the soft heating textile exhibited stable performance under distorting, making it effective for wearable applications such as wound healing and drug delivery when affixed on human wrist (Figure 5e,f). Besides, a high-temperature heating textile (15 × 7 cm^2) was also fabricated by weaving the fibers with heat-resistant Kevlar threads (Figure S12, Supporting Information). The saturated temperature reached over 160 °C at 18 V (Figure S13, Supporting Information), and the water in a 100 mL beaker was boiled by wrapping the high-temperature heating textile around it (Figure 5g,h).

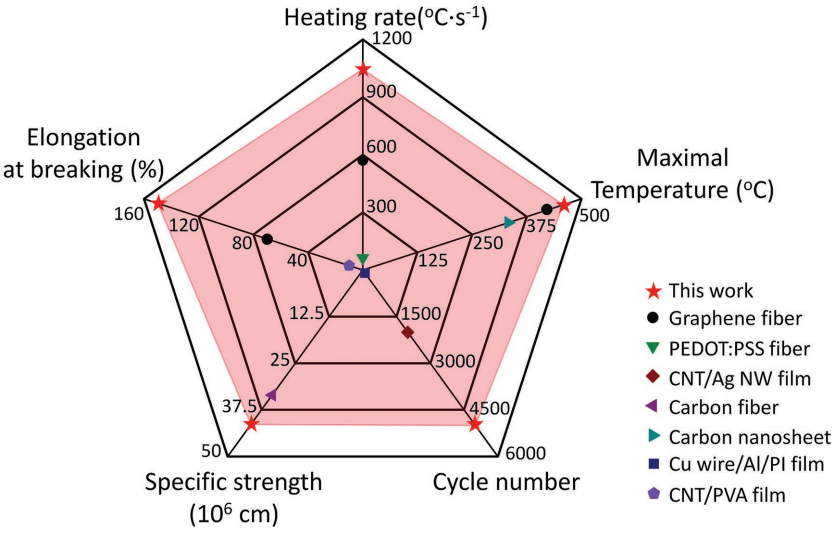

Figure 4. Comparison of the HHF with the other resistive heaters. Ag NW, silver nanowire; PI, polyimide; PVA, poly(vinyl alcohol).

In summary, we created a new family of heating fibers by designing hierarchically helical structure that offered both high stretchability and heating properties due to the formation of hierarchically helical voids. They showed many interesting and promising advantages including ultrafast thermal

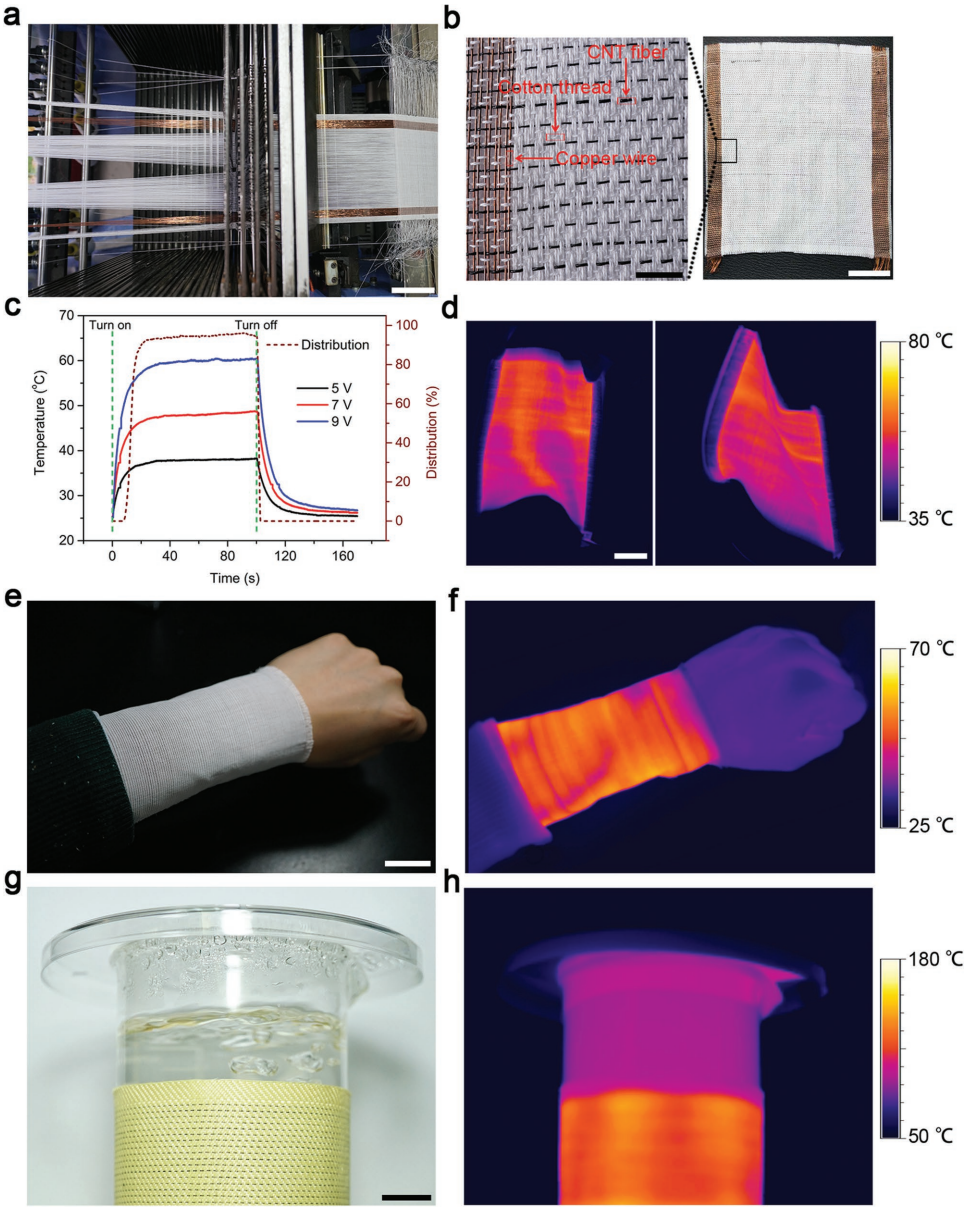

Figure 5. Production and characterization of the heating textile. a) Photograph of the producing process on loom. Scale bar, 6 cm. b) Photograph of the heating textile at high and low magnifications. Scale bar, 3 mm for the left and 25 mm for the right. c) Temperature–time and distribution–time curves of the heating textile. d) Infrared images of the heating textile under distorting at 9 V. Scale bar, 2 cm. e,f) Photograph and infrared image of the heating textile wrapped on the wrist at 9 V. Scale bar, 2.5 cm. g,h) Photograph and infrared image demonstrating that the high temperature heating textile was boiling the water at 18 V. Scale bar, 1 cm.

response, low operation voltage, and superb heating stability. In addition, such heating fibers could be easily woven into flexible and stretchable textiles at a large scale. The heating textile was soft, tough, and lightweight with outstanding heating properties. This work also opens up a new direction in the development of flexible and stretchable electronics.

Experimental Section

Preparation of Primary CNT Fibers: The CNT ribbons were synthesized by floating catalyst chemical vapor deposition method. In a reducing hydrogen atmosphere, the CNTs formed aerogel in the hot zone of a furnace (1200 °C) and the aerogel was collected into cylindrical hollow socks. The CNT sock was pulled out of the furnace by a titanium rod and then densified through water. The CNT sock shrank immediately into CNT ribbon upon arriving at the water surface. It was then washed by acetone for further densification, followed by drying, twisting, and collecting onto a spool to produce the primary CNT fibers (typical diameter of 50 μm).

Preparation of HHF: A bundle of primary CNT fibers (numbers of 5, 10, and 15) were fixed in parallel with one end stabilized at a rotating motor shaft and the other at a movable paper slip. They were then twisted at a rotary speed of 200 rpm for about 30 s. They became compact with the helixes generated along the axial direction. Typically, they produced a hierarchically helical CNT fiber with the helix density of ≈125, 90, and 70 helixes cm^{-1} for diameters of 140, 220, and 290 μm, respectively.

Fabrication of the Heating Textile: The textile was woven in plain weave on a rapier loom with width of 40 cm (Tong Yuan Textile Machinery Co., Ltd), the copper wire with cotton thread (40 S/2) was used as warp and the CNT fiber with cotton thread (ratio of 1/2) was used as weft. A piece of textile with the heating area of 10×13 cm^2 was cut out as the model.

Characterization of the Heating Textile: The human subject (Dr. P. Liu) involved in the experiments took part with informed signed consent.

Supporting Information

Supporting Information is available from the Wiley Online Library or from the author.

Acknowledgements

P.L. and Y.L. contributed equally to this work. This work was supported by Ministry of Science and Technology of the People's Republic of China (MOST) (2016YFA0203302), National Natural Science Foundation of China (NSFC) (21634003, 51573027, 51403038, 51673043, and 21604012), Science and Technology Commission of Shanghai Municipality (STCSM) (16JC1400702, 15XD1500400, 15JC1490200, and 17QA1400400), and China Postdoctoral Science Foundation (KLH1615159).

Conflict of Interest

The authors declare no conflict of interest.

Keywords

carbon nanotubes, flexible, heating fibers, stretchable, textiles

Received: August 24, 2017
Revised: September 28, 2017
Published online: November 29, 2017

[1] S. E. Naleway, M. M. Porter, J. McKittrick, M. A. Meyers, *Adv. Mater.* **2015**, *27*, 5455.
[2] G. Zan, Q. Wu, *Adv. Mater.* **2016**, *28*, 2099.
[3] Y. Forterre, J. Dumais, *Science* **2011**, *333*, 1715.
[4] L. Liu, L. Zhang, S. M. Kim, S. Park, *Nanoscale* **2014**, *6*, 9355.
[5] R. D. Farahani, K. Chizari, D. Therriault, *Nanoscale* **2014**, *6*, 10470.
[6] P. Chen, Y. Xu, S. He, X. Sun, S. Pan, J. Deng, D. Chen, H. Peng, *Nat. Nanotechnol.* **2015**, *10*, 1077.
[7] W. S. Simpson, G. Crawshaw, *Wool: Science and Technology*, CRC Press, Cambridge, England **2002**.
[8] D. Son, J. Lee, S. Qiao, R. Ghaffari, J. Kim, J. E. Lee, C. Song, S. J. Kim, D. J. Lee, S. W. Jun, S. Yang, M. Park, J. Shin, K. Do, M. Lee, K. Kang, C. S. Hwang, N. Lu, T. Hyeon, D.-H. Kim, *Nat. Nanotechnol.* **2014**, *9*, 397.
[9] B. W. An, E.-J. Gwak, K. Kim, Y.-C. Kim, J. Jang, J.-Y. Kim, J.-U. Park, *Nano Lett.* **2016**, *16*, 471.
[10] H. Lee, T. K. Choi, Y. B. Lee, H. R. Cho, R. Ghaffari, L. Wang, H. J. Choi, T. D. Chung, N. Lu, T. Hyeon, S. H. Choi, D.-H. Kim, *Nat. Nanotechnol.* **2016**, *11*, 566.
[11] S. Hong, H. Lee, J. Lee, J. Kwon, S. Han, Y. D. Suh, H. Cho, J. Shin, J. Yeo, S. H. Ko, *Adv. Mater.* **2015**, *27*, 4744.
[12] A. M. Hussain, E. B. Lizardo, G. A. T. Sevilla, J. M. Nassar, M. M. Hussain, *Adv. Healthcare Mater.* **2015**, *4*, 665.
[13] R. Wang, Z. Xu, J. Zhuang, Z. Liu, L. Peng, Z. Li, Y. Liu, W. Gao, C. Gao, *Adv. Electron. Mater.* **2016**, *3*, 1600425.
[14] D. Janas, K. K. Koziol, *Carbon* **2013**, *59*, 457.
[15] A. Laforgue, *J. Mater. Chem.* **2010**, *20*, 8233.
[16] A. Laforgue, L. Robitaille, *Macromolecules* **2010**, *43*, 4194.
[17] Y. D. Suh, J. Jung, H. Lee, J. Yeo, S. Hong, P. Lee, D. Lee, S. H. Ko, *J. Mater. Chem. C* **2017**, *5*, 791.
[18] S. Han, S. Hong, J. Yeo, D. Kim, B. Kang, M.-Y. Yang, S. H. Ko, *Adv. Mater.* **2015**, *27*, 6397.
[19] H. Sun, Z. Xu, C. Gao, *Adv. Mater.* **2013**, *25*, 2554.
[20] Y. Shang, C. Hua, W. Xu, X. Hu, Y. Wang, Y. Zhou, Y. Zhang, X. Li, A. Cao, *Nano Lett.* **2016**, *16*, 1768.
[21] L. Tan, M. Zeng, Q. Wu, L. Chen, J. Wang, T. Zhang, J. Eckert, M. H. Rümmeli, L. Fu, *Small* **2015**, *11*, 1840.
[22] Y. H. Yoon, J. W. Song, D. Kim, J. Kim, J. K. Park, S. K. Oh, C. S. Han, *Adv. Mater.* **2007**, *19*, 4284.
[23] Z. Xu, C. Gao, *Acc. Chem. Res.* **2014**, *47*, 1267.
[24] B. Fang, L. Peng, Z. Xu, C. Gao, *ACS Nano* **2015**, *9*, 5214.
[25] Z. Li, Z. Liu, H. Sun, C. Gao, *Chem. Rev.* **2015**, *115*, 7046.
[26] S. Ding, J. Jiu, Y. Gao, Y. Tian, T. Araki, T. Sugahara, S. Nagao, M. Nogi, H. Koga, K. Suganuma, H. Uchida, *ACS Appl. Mater. Interfaces* **2016**, *8*, 6190.
[27] Y. Wang, C. Zhu, R. Pfattner, H. Yan, L. Jin, S. Chen, F. Molina-Lopez, F. Lissel, J. Liu, N. I. Rabiah, Z. Chen, J. W. Chung, C. Linder, M. F. Toney, B. Murmann, Z. Bao, *Sci. Adv.* **2017**, *3*, e1602076.
[28] X.-H. Zhong, Y.-L. Li, Y.-K. Liu, X.-H. Qiao, Y. Feng, J. Liang, J. Jin, L. Zhu, F. Hou, J.-Y. Li, *Adv. Mater.* **2010**, *22*, 692.
[29] P. Liu, Z. Fan, A. Mikhalchan, T. Q. Tran, D. Jewell, H. M. Duong, A. M. Marconnet, *ACS Appl. Mater. Interfaces* **2016**, *8*, 17461.
[30] P. Liu, L. Liu, Y. Wei, K. Liu, Z. Chen, K. Jiang, Q. Li, S. Fan, *Adv. Mater.* **2009**, *21*, 3563.
[31] F. Xu, Y. Zhu, *Adv. Mater.* **2012**, *24*, 5117.
[32] X. Zhang, Q. Li, T. G. Holesinger, P. N. Arendt, J. Huang, P. D. Kirven, T. G. Clapp, R. F. DePaula, X. Liao, Y. Zhao, L. Zheng, D. E. Peterson, Y. Zhu, *Adv. Mater.* **2007**, *19*, 4198.
[33] J. Zhou, M. Mulle, Y. Zhang, X. Xu, E. Q. Li, F. Han, S. T. Thoroddsen, G. Lubineau, *J. Mater. Chem. C* **2016**, *4*, 1238.
[34] H. Souri, S. J. Yu, H. Yeo, M. Goh, J.-Y. Hwang, S. M. Kim, B.-C. Ku, Y. G. Jeong, N.-H. You, *Rsc. Adv.* **2016**, *6*, 52509.
[35] P. Li, J. Ma, H. Xu, X. Xue, Y. Liu, *J. Mater. Chem. C* **2016**, *4*, 3581.
[36] D. Kim, L. Zhu, D.-J. Jeong, K. Chun, Y.-Y. Bang, S.-R. Kim, J.-H. Kim, S.-K. Oh, *Carbon* **2013**, *63*, 530.
[37] J. T. Han, S. Choi, J. I. Jang, S. K. Seol, J. S. Woo, H. J. Jeong, S. Y. Jeong, K.-J. Baeg, G.-W. Lee, *Sci. Rep.* **2015**, *5*, 9300.

